Rev. LatinAm. Metal. Mat.

Artículo Regular

www.rlmm.org

WETTING TRANSITIONS ON THE SUBMERGED METAL MATRIX COMPOSITE SURFACE

Reza Kianifard[1*] *and Isar Behckam*[2]

1: Mechanical engineering department, Islamic Azad University - Shoushtar, Shoushtar, Iran
2: Material engineering department, Iran University of Science and Technology, Tehran, Iran

**e-mail: r.kianifard@iau-shoushtar.ac.ir*

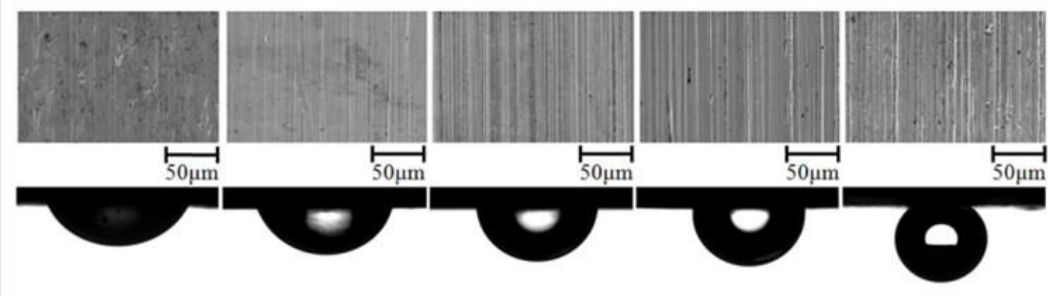

ABSTRACT

The wetting transition is studied for the oil droplets placed on the underwater surface of metal matrix composites. Oil penetration into the cavities between the asperities is accompanied by a change in the contact angle and may result in the Cassie-Wenzel transitions. Experimental data of contact angles of oil-air, water-air, and oil-water systems on the surface of aluminum-graphite composites are collected. The Wenzel-Cassie wetting transition is revealed by increasing the roughness for various aluminum-graphite samples. A theoretical model is proposed to verify the effect of surface topography and roughness on the wetting transitions.

Keywords: Underwater Wetting Transitions, Superhydrophobicity, Oleophobicity, Oleophilicity.

TRANSICIONES EN EL MOJADO DE LA SUPERFICIE DE UN MATERIAL COMPUESTO DE MATRIZ METÁLICA

RESUMEN

Se estudia la transición en el mojado para gotas de aceite colocadas en una superficie sumergida bajo agua de un material compuesto de matriz metálica. La penetración del aceite en las cavidades que se forman entre las asperezas de la superficie se ve acompañada por un cambio en el ángulo de contacto y puede resultar en transiciones Cassie-Wenzel. Se recolectaron datos experimentales de ángulos de contacto en sistemas aceite-aire, agua-aire y aceite-agua sobre la superficie de un material compuesto de matriz metálica aluminio-grafito. La transición de mojado Wenzel-Cassie se revela al incrementar la rugosidad superficial de varias muestras del material compuesto aluminio-grafito. Se propone modelo teórico para verificar el efecto de la topografía superficial y la rugosidad en dichas transiciones de mojado.

Palabras clave: Transiciones de mojado bajo el agua, superhidrofobicidad, oleofobicidad, oleofilicidad.

Recibido: 17-09-2013 ; **Revisado:** 28-10-2013
Aceptado: 31-10-2013 ; **Publicado:** 11-11-2013

pISSN: 0255-6952 | eISSN: 2244-7113
Rev. LatinAm. Metal. Mat. 2014; **34** (2): 282-288

1. INTRODUCTION

Wetting and superhydrophobicity have attracted the attention of researchers since the new technologies emerged to produce surfaces with designed microstructure and also because of the need to design nonwetting, nonsticky, oleophobic, omniphobic, and self-cleaning surfaces.

Furthermore, the necessity of the superhydrophobicity to fabricate anti-icing surface has been recently studied and the correlations between hydrophobicity and reduction of ice-adhesion have been reported.[1-3] Although the prevention of ice formation has been related to superhydrophobicity, it is still controversial whether superhydrophobic surfaces are the best to be used to design anti-icing surfaces.[4-7]

The primary parameter that characterizes the wetting of solid surfaces is contact angle. Contact angle of a droplet on a smooth solid surface can be obtained by the Young equation as

$$\cos\theta_0 = \frac{\sigma_{SA}-\sigma_{SL}}{\sigma_{LA}} \qquad (1)$$

where θ_0 is the contact angle of the droplet on the smooth surface and σ_{SL}, σ_{SA} and σ_{LA} are the surface energies of solid-liquid, solid-air, and liquid-air interfaces. However, in practice most surfaces are rough to some extent and it is well understood that the wetting of rough and smooth surfaces are different. When water contact angle exceeds 90°, this is referred to as hydrophobicity, otherwise referred to as hydrophilicity. When a surface repels oils or any organic liquids, it is called oleophobic. The term oleophobicity can be applied to a three-phase interface of solid, oil, and air, and also to a three-phase solid-oil-water interface (underwater oleophobicity). Surface roughness magnifies the oleophobicity, bringing the contact angle into the superoleophobic region where the contact angle is between 150° and 180°. It is realized that the single value of contact angle cannot completely characterize the wetting but a range of value between advancing and receding contact angle is needed. The difference between the advancing and receding contact angle is called "contact angle hysteresis". Originally, contact angle hysteresis was associated with surface contaminants. Besides high contact angle, superoleophobic surfaces also usually have low contact angle hysteresis, and show self-cleaning properties.[8-10] Dorrer and Ruhi[11] determined the advancing and receding contact angles as a function of the roughness geometry. They observed that a surface with high static contact angle still require a low contact angle hysteresis to show superhydrophobic properties. Forsberg et al.[12] reveal that pinning on surface roughness can give very high static advancing contact angles in the Wenzel state.

A significant amount of research work was done on design, fabrication, and characterization of superhydrophobic and superoleophobic surfaces from various materials, ranging from polymers and ceramics to textiles. Nosonovsky et al.[13] studied the relationship between the local roughness and contact angle of water droplets on metal matrix composites (MMCs), finding that the contact angle can increase with increasing roughness. Marmur[14] theoretically interpreted the superhydrophobicity mechanism of the lotus leaf. Gao and McCarthy[15] investigated the contact angle hysteresis and claimed that the main reason for contact angle hysteresis is the pinning point of the receding contact angle by the post tops of the surface. Jung and Bhushan[16] studied the wetting behavior of water and oil droplets for hydrophobic/hydrophilic and oleophobic/oleophilic surfaces in three-phase interface. Ohkubo et al.[17] presented a novel method to prepare oleophobic materials.

Besides hydrophobicity and oleophobicity, wetting transitions have been precisely studied recently due to their relevance and importance for the oleophobicity. Although wetting transitions on superhydrophobic surfaces are well studied, much less attention has been given to the wetting transition during the contact of organic liquids like oils with rough solid surfaces. Hejazi and Nosonovsky[18] studied the wetting transition of various interfaces of solid-water, solid-water-air, and solid-oil-water-air. Shirtcliffe et al.[19] showed that a transition from Wenzel to Cassie-Baxter is likely for rough and patterned surfaces of copper. They found that the contact angle hysteresis on these surfaces initially increased and then decreased as the contact angle increased. Bormashenko[20] reviewed the main experimental and theoretical approaches to wetting transitions. Hejazi et al.[21] investigated the underwater wetting transition on oleophobic surface of brass.

The basic theoretical model regarding the wetting of rough surfaces was proposed by Wenzel[22] and then

developed by Cassie-Baxter[23]. According to the Wenzel model (Fig. 1a), water penetrates into the cavities between the asperities and the contact between solid and water is complete, therefore increase in roughness causes increase in the area of solid-liquid interface, which results in higher and lower contact angle for an intrinsically hydrophobic and hydrophilic surface, respectively. However, according to the Cassie-Baxter model (Fig. 1b), the air can be trapped into the cavities which makes partial contact of solid and water.

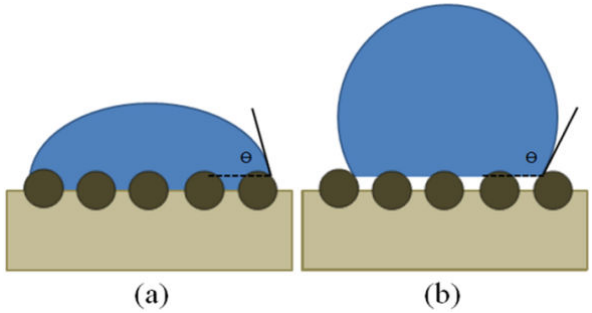

Figure 1. Schematic of the (a) Wenzel and (b) Cassie-Baxter regimes.

In this paper we present a model showing the topography of immersed aluminum-graphite composite surface and experimentally investigate the effect of surface roughness on wetting transition. The model can be used to study wetting transitions in underwater oleophobic systems, which are discussed in consequent sections. We also show that roughening an underwater solid surface can cause the transition from Wenzel to Cassie–Baxter state.

2. THEORY

In this section, we present our modeling of surface topography of immersed aluminum-graphite composite surface. Depending on the properties of a particular system, including surface roughness and interfacial energies, different phase interface can form. We apply the same model as Hejazi and Nosonovsky[24] used for metal matrix composites. They assumed the graphite particles are spherical protrusions that make roughness on the surface (Fig. 2).

Considering a section of matrix including randomly distributed particles with radii r (Fig. 2), the reinforcements volume fraction, f_v, is obtained through dividing the total volume of all particles inside the section, V_r, by the volume of section, V_t,

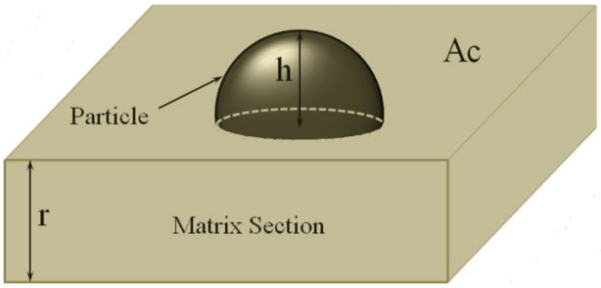

Figure 2. The schematic of a matrix section including spherical particles.

$$f_v = \frac{Vr}{V_t} \quad (2)$$

$$V_r = \frac{4n\pi r^3}{3} \quad (3)$$

$$V_t = A_t.r \quad (4)$$

where A_t is the top surface of the section and n is the total number of particles inside the section. Substituting Eqs. 3 and 4 into Eq. 2 gives

$$n = \frac{3f_v V_t}{4\pi r^3} \quad (5)$$

The projection height of the particle out of matrix section is defined by h. Since the metal matrices usually are softer than reinforcements, h can be changed due to wear. We assumed that $0 \le h \le r$ (Fig. 3).

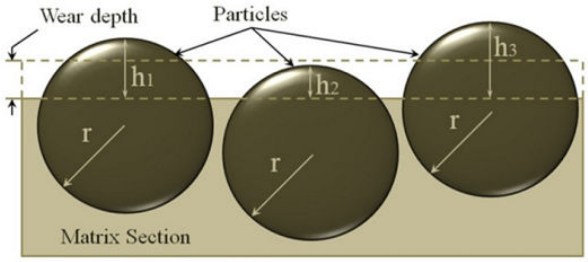

Figure 3. The schematic of changing h due to wear.

Therefore,

$$f_r = \frac{A_r}{A_t} \quad \rightarrow \quad f_r = \frac{3}{4} f_v \quad (6)$$

where f_r is the fractional reinforcement area. The total area of reinforcements, A_r, in contact area, can be calculated as

$$A_r = n\left(\frac{1}{r}\int_0^r 2\pi r h\, dh\right) = n\pi r^2 \quad (7)$$

Fractional area of matrix, f_m, can be calculated from the following equation

$$f_m + f_r = 1 \quad \rightarrow \quad f_m = 1 - \frac{3}{4} f_v \tag{8}$$

The averaged Wenzel roughness factor is defined as

$$\frac{1}{R_f} = 1 - \frac{A_r}{4A_t} \quad \rightarrow \quad \frac{1}{R_f} = 1 - \frac{3}{16} f_v \tag{9}$$

Combining the Wenzel and Cassie-Baxter equations gives the contact angle on a composite surface, θ

$$\cos\theta = R_f f_r \cos\theta_r + f_m \cos\theta_m \tag{10}$$

Substituting Eqs. 6, 8 and 9 into Eq. 10 yields

$$\theta = \cos^{-1}\left[\frac{12 f_v}{16 - 3 f_v} \cos\theta_r - \frac{3}{4} f_v \cos\theta_m + \cos\theta_m\right] \tag{11}$$

Then we used the equation for the case when the reinforcements and matrix are made by graphite particles and aluminum, respectively. According to our experiments, the contact angle of oil droplet with relatively pure graphite and aluminum are about 120 and 45 degree, respectively. Fig. 4 shows the contact angle of oil droplet on surface of aluminum matrix composite reinforced by graphite particles versus reinforcement volume fraction obtained from the equation 11. It is observed that the contact angle increases with increasing the reinforcement volume fraction.

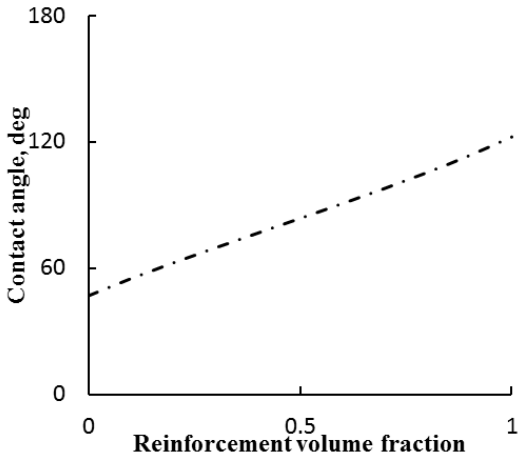

Figure 4. Contact angle of oil droplet versus graphite particles volume fraction in metal matrix.

3. EXPERIMENTAL PART

In order to verify the model described in the preceding section, experiments with metal matrix composites were performed and the oleophobicity of five 20×20×5 mm samples of aluminum-graphite composites with different roughness immersed in water was studied experimentally. We used aluminum because it is easy to work with and inexpensive. Distilled water and regular pure vegetable oil were used as the evaluation media. The contact angles with a smooth surface for the solid-water-air, solid-oil-air, and solid-oil-water system are 60° , 30° , and 45° , respectively. The aluminum-graphite samples were washed and cleaned with deionized water and then were grinded.

A surface is known to be roughened on the microscale with various approaches, including chemical etching, laser etching, mechanical abrasion, etc. Here the samples were mechanically abraded through successive grinding steps with 80, 200, 400, 600, and 1200 grit silicon carbide papers, and then to remove debris, they were polished with a soft cloth impregnated with 1 μm silica particles. Finally, the polished samples with various surface roughness were dried in air.

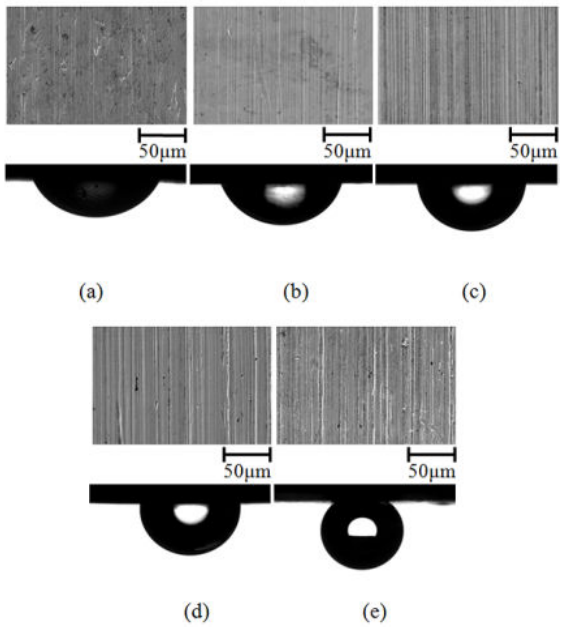

Figure 5. SEM of samples and underwater oil droplet images on Aluminum-graphite composites abraded with SiC paper with a particle size of a) 5 μm, b) 15 μm, c) 26 μm, d) 46 μm, e) 82μm, and abraded with soft cloth (1 μ m particle size).

We measured the surface roughness of all samples with a surface tester/profilometer (Mitutoyo 178 Portable). The average roughness values, R_a, measured by the profilometer are 3.5, 2.7, 2.0, 1.0 and 0.1 μm. The scanning electron microscope (SEM) images of the polished samples are as shown in Fig. 5.

We measured the contact angle of deionized water and vegetable oil droplets in air and for oil droplets in water deposited on the aluminum surfaces using a model 500 ramé-hart goniometer. For measuring the contact angle of solid-oil-water system, we immersed samples horizontally in a water chamber. Since the density of vegetable oil used in this experiment is less than that of water, we placed the oil droplet on the surface bottom using a U-type inverted needle. The volume of droplets is about 7 μl. We placed 3 oil droplets on different locations of each sample and averaged the results in order to reduce the errors in measurements. Figure 5 shows the oil droplets deposited on samples immersed in water.

4. RESULTS AND DISCUSSION

Fig. 6 represents the contact angle of water and oil droplets on aluminum-graphite samples in air with various average roughness, R_a, and also the contact angle of oil droplet placed on the aluminum-graphite samples immersed in water. It is observed that the values of water and oil contact angle in air do not considerably change with increasing R_a. However for an oil droplet in water, the contact angle increases when average roughness, R_a reaches the 1.0 μm. The values of the contact angle increase abruptly from 50° to 120°. The steep increase of the contact angle and the change of the wetting regime from oleophilic to oleophobic reveals that a wetting transition from the Wenzel to Cassie-Baxter regime. The change in contact angle of the droplets shown in figure 5 also validate this transition.

We measure the advancing and receding contact angles of oil on the water-immersed samples as well as the contact angle hysteresis to verify the accuracy of our interpretation regarding the underwater oil repellency of the samples. The results are presented in Table 1.

Fig. 7 shows the contact angle hysteresis for oil-air (O-A), water-air (W-A), and oil-water (O-W) systems on the surface of aluminum-graphite composites.

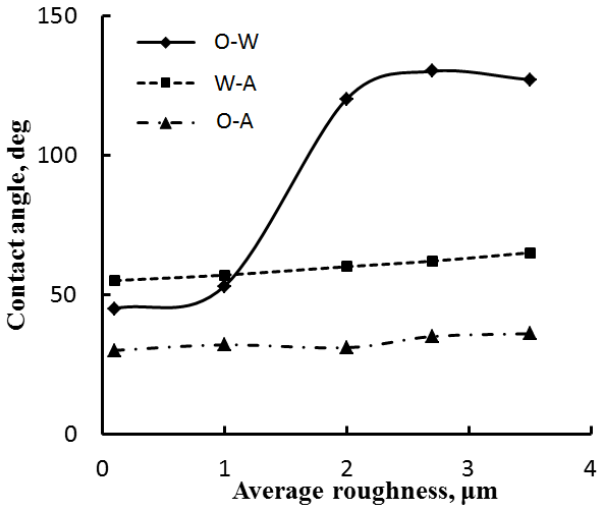

Figure 6. Underwater oil droplet, water droplet and oil droplet in air contact angles of samples as a function of the average roughness, R_a.

Table1. Advancing, receding and contact angle hysteresis of the samples.

	Sample1 *Ra=0.1μm*	*Sample2* *Ra=1μm*	*Sample3* *Ra=2μm*	*Sample4* *Ra=2.7μm*	*Sample5* *Ra=3.5μm*
Adv. CA	58	64	137	144	140
Rec. CA	41	46	128	138	133
Hysteresis	17	18	9	6	7

In the Wenzel regime, the contact angle for a rough surface, θ_W , is given by

$$\cos\theta_W = R_f \cos\theta_0 \qquad (12)$$

where R_f is the roughness factor defined as a ratio of the surface area to its flat projection and θ_0 is the contact angle of the droplet with a smooth surface. Note that both R_f and R_a are the measures of surface roughness; however, $R_f \geq 1$ is a nondimensional parameter, and $R_f = 1$ for a smooth surface, whereas $R_a \geq 0$ is a dimensional parameter, and $R_a = 0$ μm for a perfectly smooth surface. It is however expected that increasing R_a corresponds to increasing R_f. The

relationship between R_a and R_f is not straightforward. Considering the geometrical properties of the surface, we assumed that $R_f = (R_a/(0.3 + 3R_a)) + 1$. According to equation 12, for initially oleophilic surface ($\cos\theta_0 > 0$), increasing roughness cannot result in the transition to oleophobicity ($\cos\theta_W < 0$). Therefore, the regime change from the oleophilicity to oleophobicty observed in figure 6 cannot be explained by the Wenzel model. In the CB regime, the contact angle for a rough surface, θ_{CB} , is given by

$$\cos\theta_{CB} = f_{SO}(R_f \cos\theta_0 + 1) - 1 \qquad (13)$$

where θ_0 is the contact angle of an oil droplet in water with a smooth solid surface, R_f is the roughness factor applied to the solid-oil contact area, and f_{SO} is the fractional solid-oil contact area.

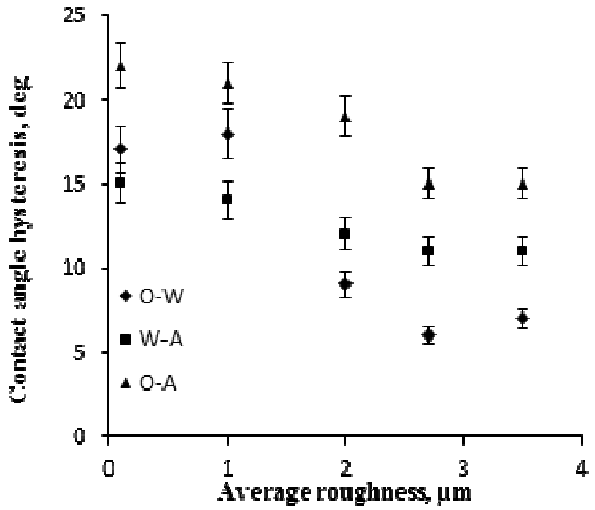

Figure 7. Contact angle hysteresis as a function of the average roughness, R_a.

It is found from equation 13 that the abrupt change of the underwater solid-oil contact angle, as reported in Fig. 8, can be attributed to the abrupt change of either f_{SO} or R_f. Roughening the surface with the sandpaper results in increasing R_a and can lead to increasing R_f. However, for a surface with a $\cos\theta_0 > 0$ (oleophilic), the increase of R_f cannot result in the change of the sign of $\cos\theta_0$ from positive (oleophilic) to negative (oleophobic). Therefore, the only plausible explanation to the above-mentioned abrupt growth of the oil contact angle underwater from 50° to 120° is an abrupt change of the solid-oil contact area, f_{SO}. A rougher surface has larger cavities so that air or water pockets can be trapped between the solid surface and oil droplet.

The value of f_{SO} can be calculated as

$$f_{SO} = \begin{cases} -0.17R_a + 1 & 0 \le R_a < 1 \\ -0.6R_a + 1.43 & 1 \le R_a < 2 \\ -0.02R_a + 0.27 & 2 \le R_a < 3.5 \\ 0.2 & R_a \ge 3.5 \end{cases} \qquad (14)$$

Whether the air pockets are present in the system, in addition to water pockets, depends on the history of the system, i.e., how water and oil were introduced. In a solid-water system (turned upside down for contact angle measurements), air is likely to be trapped between the solid and water. When oil is accurately introduced into the system with an inverted needle, the air bubbles can remain at the interface. On the other hand, if oil is introduced first, it is likely to fill the cavities with no air pockets. Note that f_{SO} = 1 corresponds to the Wenzel regime and an abrupt drop of the contact area from f_{SO} = 1 indicates the wetting transition from Wenzel to Cassie-Baxter regime. The values of the contact angle of oil with a solid in water are presented in Fig. 8 as calculated from the Wenzel (Equation 12) and Cassie-Baxter (Equation 13) models.

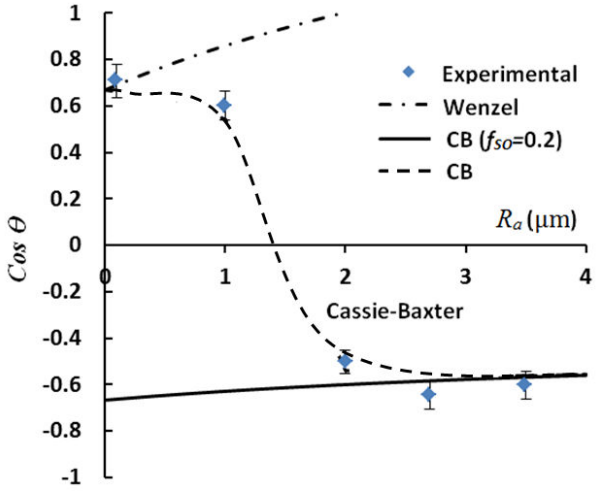

Figure 8. Underwater oil contact angle versus surface roughness, R_a, for W, CB with a constant solid-oil contact area fraction (f_{SO} = 0.2), and CB with solid-oil contact area fraction dependent on roughness.

5. CONCLUSIONS

In summary, we investigated wetting of rough aluminum-graphite composite surfaces by water and oil in air, as well as oil in water. We found an abrupt increase of the contact angle for the oil underwater system. The increase cannot be explained by the standard Wenzel and Cassie–Baxter models; however, it is consistent with the wetting regime change (wetting transition) from Wenzel to Cassie-Baxter. Such non-wetting transitions are known for superhydrophobic surfaces; however, we report for the first time about such transition for wetting of an aluminum-graphite surface with an organic nonpolar liquid.

6. REFERENCES

[1]. R. Jafari, R. Menini, M. Farzaneh, Applied Surface Science 257 (2010) 1540

[2]. R. Menini, Z. Ghalmi, M. Farzaneh, Cold Regions Science and Technology 65 (2011) 65

[3]. P. Guo, Y. Zheng, M. Wen, C. Song, Y. Lin, L. Jiang, Advanced Materials 24 (2012) 2642

[4]. A. J. Meuler, G. H. McKinley, R. E. Cohen, ACSNano 4 (2010) 7048

[5]. M.Nosonovsky, V. Hejazi, ACSNano 6 (2012) 8488

[6]. S. A. Kulinich, S. Farhadi, K. Nose, X. W. Du, Langmuir 27 (2011) 25

[7]. V. Hejazi, M. Nosonovsky, Scientific reports 3 (2013a) DOI:10.1038/srep02194

[8]. Y. C. Jung, B. Bhushan, Nanotechnology 17 (2006) 4970

[9]. V. Hejazi, M. Nosonovsky, Colloid and Polymer Science 291 (2013b) 329

[10]. V. Mortazavi, V. Hejazi, R. M. D'Souza, M. Nosonovsky in Advances in Contact Angle, Wettability and Adhesion, K. L. Mittal, Scrivener, NY, USA, 2013, Vol.1.

[11]. C. Dorrer, and J. Rühe, Langmuir 24 (2008) 1959.

[12]. P.S.H. Forsberg, C. Priest, M. Brinkmann, R. Sedev, J. Ralston, Langmuir 26 (2010) 860.

[13]. M. Nosonovsky, V. Hejazi, A. E. Nyong, P. K. Rohatgi, Langmuir 27 (2011) 14419

[14]. A.Marmur, Langmuir 20 (2004) 3517

[15]. L. Gao, T. J. McCarthy, Langmuir 22 (2006) 2966

[16]. Y. C. Jung, B. Bhushan, Langmuir 25 (2009) 14165

[17]. Y. Ohkubo, I. Tsuji, S. Onishi, K. Ogawa, J. Mater. Science 45 (2010) 4963

[18]. V. Hejazi, M. Nosonovsky, Langmuir 28 (2012a) 2173

[19]. N. J. Shirtcliffe , G. McHale, M. I. Newton, C. C. Perry, Langmuir 21 (2005) 937

[20]. E. Bormashenko, Philos. Trans. R. Soc. London, Ser. A, 368 (2010) 4695

[21]. V. Hejazi, A. E. Nyong, P. K. Rohatgi, M. Nosonovsky, Advanced Materials, 24 (2012) 5963

[22]. R. Wenzel, Ind. Eng. Chem. 28 (1936) 988

[23]. A. B. D. Cassie, S. Baxter, Trans. Faraday Soc., 40 (1944) 546

[24]. V. Hejazi, M. Nosonovsky, in Green Tribology, Biomimetics, Energy Conservation and Sustainability, M. Nosonovsky, B. Bhushan, Springer, Heidelberg, Germany, (2012b), p. 149.